A Numerical Study of the Paraxial Wave Equation

Svetlana Avramov-Zamurovic
Department of Weapons, Robotics and Control

Kyle Jung and Reza Malek-Madani
Department of Mathematics

US Naval Academy, Annapolis, MD 21402

Abstract

In this paper we apply COMSOL to obtain a numerical solution to an initial-boundary value problem (IBVP)for the paraxial wave equation (PWE). This equation arises in laser beam propagation in a cylindrical cavity. We compare the finite-element solution we obtain from COMSOL to the Galerkin approximation solution of the same problem. Finally, we compare these two approximate solutions to the exact solution of the PWE in free space and discuss similarities and differences.

1 Introduction

The Paraxial Wave Equation

$$U_{xx} + U_{yy} + 4iMU_z = 0 \tag{1}$$

is a well-known reduced model governing the propagation of laser beams (see [1], Chapter 4, for a dimensional version of this equation). The function U in (1) is any component of the electric or the magnetic fields of the beam, and M is a non-dimensional parameter defined in terms of the various parameters that define the laser beam.[1]

It is more convenient to work with the real and imaginary parts of the solution: Let $U = V_1 + iV_2$, and note that (1) is equivalent to

$$\begin{cases} \Delta V_1 - 4M\dfrac{\partial V_2}{\partial z} &= 0, \\ \Delta V_2 + 4M\dfrac{\partial V_1}{\partial z} &= 0, \end{cases} \tag{2}$$

where $\Delta = \frac{\partial^2}{\partial x^2} + \frac{\partial^2}{\partial y^2}$. When confined to the half-space $z > 0$, the system in (2) has several exact solutions, and chief among them is the following solution that starts out as a Gaussian function at $z = 0$ and remains Gaussian for $z > 0$:

$$\begin{cases} V_1 &= \dfrac{1}{W}\exp(-\dfrac{r^2}{W^2})\cos(\phi + \dfrac{Mr^2}{F}), \\ V_2 &= -\dfrac{1}{W}\exp(-\dfrac{r^2}{W^2})\sin(\phi + \dfrac{Mr^2}{F}), \end{cases} \tag{3}$$

where $r = \sqrt{x^2 + y^2}$, and $W(z) = \sqrt{\Theta_0^2 + \Lambda_0^2}$ is called the spot radius (also called the spot size) of the beam at any z. Here $\Theta_0 = 1 - z$ and $\Lambda_0 = \frac{z}{M}$ are the refraction and diffraction parameters of the beam, respectively. Moreover, the function $\phi = \tan^{-1}\frac{\Lambda_0}{\Theta_0}$ is the phase shift, and

$$F = \frac{(\Theta_0^2 + \Lambda_0^2)(\Theta_0 - 1)}{\Theta_0^2 + \Lambda_0^2 - \Theta_0} \tag{4}$$

[1] A Gaussian laser mean typically has a waist w_0 and a phase radius of curvature F_0. In terms of these parameters and the light's wavenumber k, M is defined as $\frac{kw_0^2}{2F_0}$.

is the radius of curvature of the beam's phase at any z. When F is positive, the beam is converging, and diverging when F is negative. In the special case when F is unbounded (infinity), the beam is said to be collimated. This exact solution will guide us throughout this paper where our main goal is to compute approximate solutions of (2), not in the half-space $z > 0$, but instead in a cylinder that somewhat resembles the experimental domain in which we perform beam propagation.

To that end we consider the domain Ω_a defined by

$$\Omega_a = \{(x, y, z) | x^2 + y^2 \leq a^2,\, z > 0\}. \tag{5}$$

For boundary conditions we choose Dirichlet boundary conditions for both components of U:

$$V_1|_{\partial\Omega_a} = V_2|_{\partial\Omega_a} = 0, \tag{6}$$

and for initial conditions, motivated by the value of the exact solution in (3) at $z = 0$, and modified appropriately for the bounded domain Ω, we consider

$$\left\{ \begin{array}{lcl} V_1(x, y, 0) & = & \exp(-r^2)\cos(Mr^2)g(r), \\ V_2(x, y, 0) & = & -\exp(-r^2)\sin(Mr^2)g(r). \end{array} \right. \tag{7}$$

The function g in (7) is

$$g(r) = \frac{1}{2}(1 + \cos[\pi(\frac{r}{a})^6]). \tag{8}$$

The first part of the initial conditions (the product of the exponential and the trigonometric functions) is simply the exact solution (3) evaluated at $z = 0$. The function g in (8) introduces attenuation in the bounded domain Ω, so that the initial conditions and the Dirichlet boundary conditions in (6) are compatible.

2 The Galerkin Solution

The IBVP (2), (6), and (7) has the following approximate solution:

$$V_1(x, y, z) = \sum_{n=1}^{\infty} (b_n \cos \frac{\lambda_n^2}{4M} z + c_n \sin \frac{\lambda_n^2}{4M} z)\, J_0(\lambda_n r). \tag{9}$$

$$b_n = \frac{1}{C_n} \int_0^a V_1(r, 0) J_0(\lambda_n r) r dr, \quad c_n = \frac{1}{\lambda_n^2 C_n} \int_0^a \Delta(V_2(r, 0)) J_0(\lambda_n r) r dr,$$

where

$$C_n = \int_0^a J_0(\lambda_n r)^2 r dr, \quad \lambda_n = \frac{j_{0,n}}{a}, \quad n = 1, 2, ...$$

and $j_{0,n}$ is the n-th zero of $J_0(r)$, the Bessel function of the first kind. The expression for V_2 is obtained from (2)b by first computing the laplacian of V_1 given by (9) followed by an integration in z and applying the known value of V_2 at $z = 0$.

3 Results from the Galerkin method

The figures in this section compare the analytical solution of the free space problem (the red curve) to the one obtained using the Galerkin approximation with the 100-th partial sum of (9) (the blue curve). In Figures 1–3 the horizontal axis shows values of z while on the vertical axis the quantities V_1, V_2, and $|U|$ restricted to the axis, $(x, y) = (0, 0)$, are displayed. The physical parameters used are

$$F_0 = 500\,\text{m},\ w_0 = 3\,\text{cm},\ \lambda = 633\,\text{nm},$$

resulting in the value $M = \frac{kw_0^2}{2F_0} = 8.93344$, where $k = \frac{2\pi}{\lambda}$. Each figure contains two graphs, one for a quantity in free space, and the second, the same quantity calculated using the Galerkin method.

There are a few features worth noting in these figures. First, there is a remarkable agreement between the solutions of the two regimes, where one is propagating unobstructed in free space and the other having to negotiate the effects of the boundary. By taking the boundary of the cylinder, a, relatively large, we have attempted to mitigate the effect of the boundary as much as possible, where we have succeeded to a large extent as far as the IBVP solution

at $(x, y) = (0, 0)$ is concerned. However, as soon as we look at any of the three figures at points away form the axis of propagation, see Figures 4–6, the boundary effects become quite pronounced. It is not clear, for instance, if the oscillations one sees in the IBVP solution when the points (x, y) are away from $(0, 0)$, which are typically quite a bit larger than the ones observed in Figures 1–3, are due to numerical instabilities associated with the Galerkin method, or due to the fact the Dirichlet boundary conditions cause reflections that begin to interfere with the original beam, a feature that is less noticeable on the axis of the beam.

A second feature worth noting is the location where the intensity peaks. Perhaps the fact that the size of the maximum intensity is not quite the same as the one in the free space solution is less significant than the discrepancy in the z values where the maximum occurs. This point is actually one of the main differences we have noticed when we compare the Galerkin solution to the one we obtain in COMSOL, which is the subject of the next section.

4 Results in COMSOL

We have also obtained the solution to the initial-boundary value problem (2), (6), and (7) in COMSOL. Figures 7-12 show the output of COMSOL, which should be compared to Figures 1–6. The F_0, w_0, and λ parameter values remain the same.

The initial-boundary value problem (2), (6), and (7) was setup within COMSOL's coefficient form partial differential equation module. A disk shaped geometry with a radius $a = 5$ was selected to simulate the x, y domain (5) in COMSOL. A consistent distribution of triangular shaped elements was applied to form a mesh on the domain. Our mesh consisted of 25970 elements with 52257 degrees of freedom for each dependent variable V_1 and V_2 for a total of 104512 degrees of freedom within the 2D disk. The $z > 0$ part of the domain was simulated with COMSOL's time-dependent solver using a backwards differentiation formula (BDF) solver. The solver took 18 minutes and 24 seconds to run. Figure 13 gives a convergence plot for COMSOL's time dependent solver.

Similar to the Galerkin method results, the COMSOL results reveal a resemblance to the analytical free space solution at the beam center $(x, y) = (0, 0)$. Additionally, the off-axis beam at $(x, y) = (0.1, 0.1)$ from COMSOL appear similar in shape to the Galerkin method solution, but they both differ from the free space solution, perhaps for reasons discussed earlier.

5 Conclusions

In this paper we presented a numerical study of the PWE with parameter values that are suitable for modeling laser beam propagation. Our motivation is to develop enough skill and confidence in numerical modeling of beam propagation to eventually study how laser beams propagate in turbulent media. As described in [2] (as well as in many other references that can be found at www.usna.edu/lime), this work is part of a much bigger effort to understand how to design laser beams that remain robust and stable when travelling through a turbulent medium, be it an atmospheric or an oceanic medium. The current study is a small step toward modeling the experimental setup described in [2]. Because the problem at hand inherently involves multiple physics, our goal is to use COMSOL for the ultimate problem where we need to find solutions of a system of PDEs with variable coefficients, taking into account spatially varying index of refraction changes along the propagation path, in order to model the interaction of laser beams with and fluid flows.

In this paper we compared the solution of an initial-boundary value problem obtained by a Galerkin method and by COMSOL. The solutions are similar in many respects, especially when compared with the analytical solution of the free space problem, in that both solutions have the general trends of the analytical solution. The numerical solutions are particularly good on the axis of propagation and agree well with the analytical solution there. We are especially mindful of the on-axis agreement among the various solutions because the on-axis intensity is the largest value of the beam intensity in any cross section and presumably this value is influenced less by the reflections from the boundary, especially if the boundary is kept at a distance from the beam. Nevertheless, there are discrepancies between the two numerical solutions, and these differences are pronounced enough that prompt us to continue investigating the two methods in this simple setting before embarking on using COMSOL on much more complicated models of beam propagation.

Finally, we point out that our COMSOL implementation of PWE was carried out by introducing the system of equations (2) to its PDE solver, while the bulk of the development of the Galerkin method was applied to the biharmonic equation that results by eliminating either of the two variables V_1 or V_2. In a presentation that accompanies this conference paper, the authors present the results of implementing the biharmonic solver in COMSOL and report on those results.

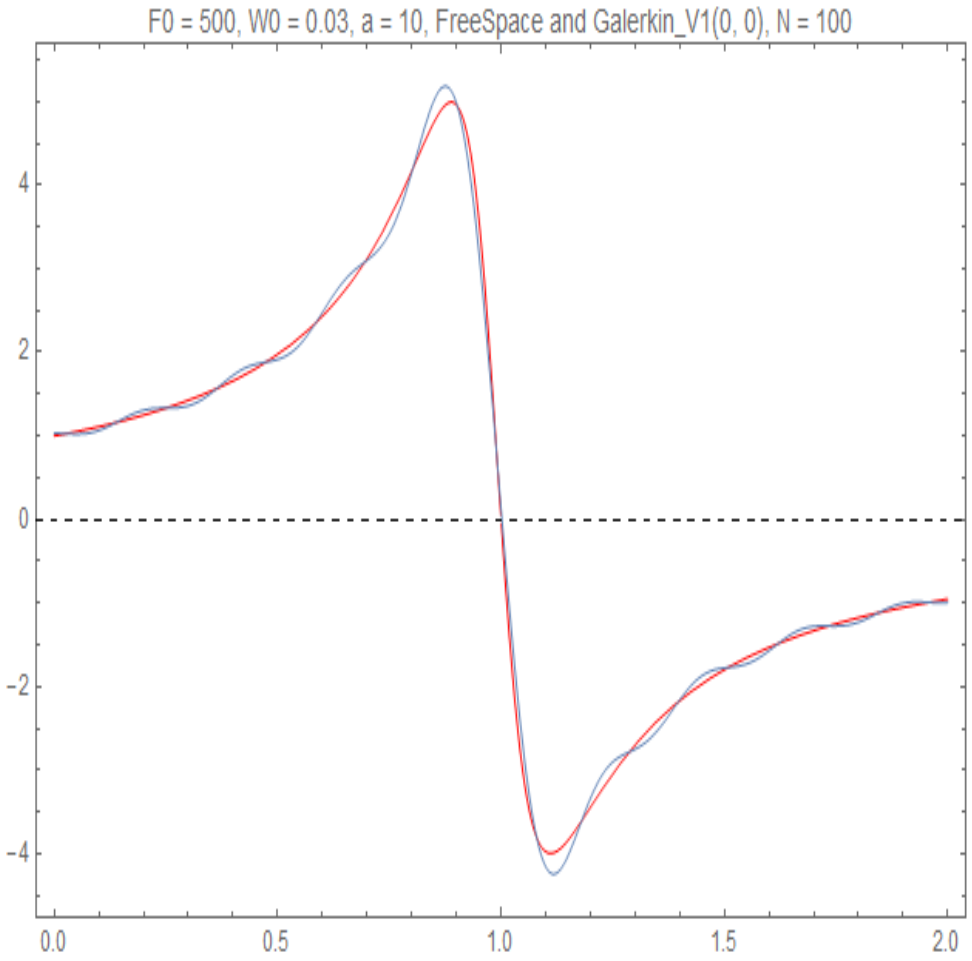

Figure 1: The two graphs in this figure are the graphs of V_1, computed two different ways, using the exact solution in free space, and in a bounded domain using 100 basis functions in the Galerkin method.

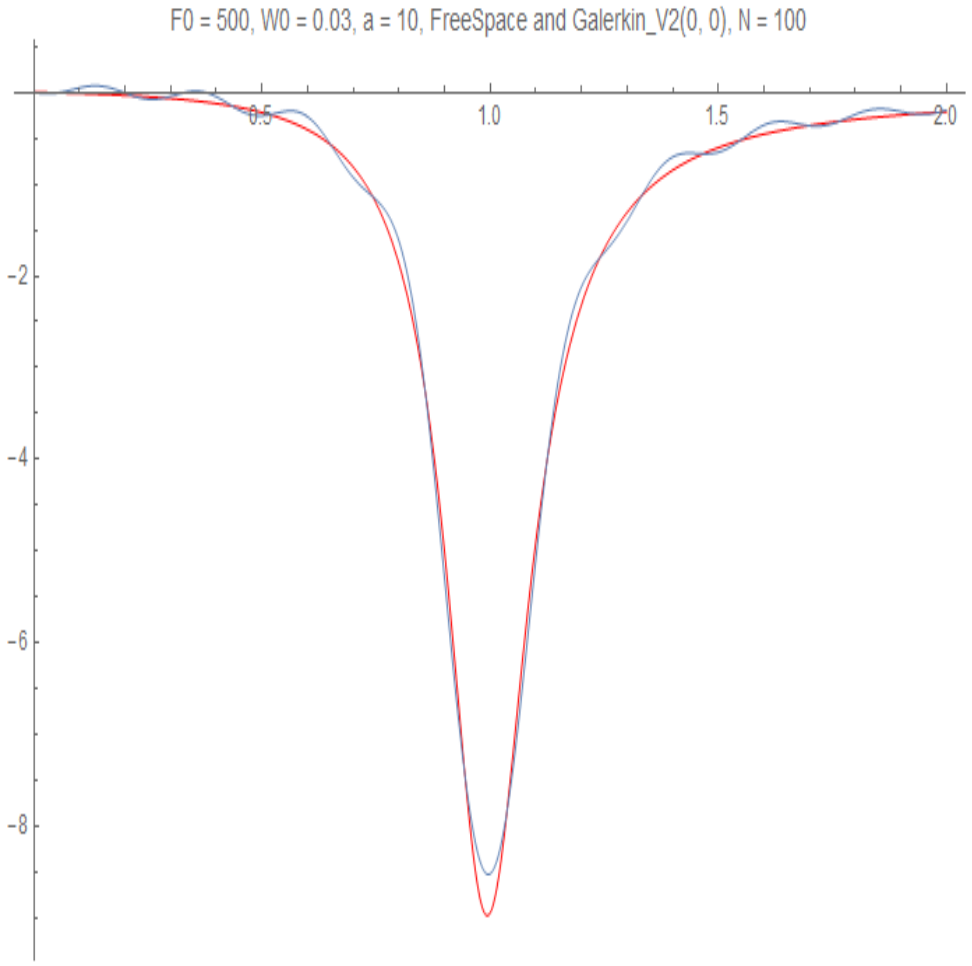

Figure 2: The two graphs in this figure are the graphs of V_2, computed as described in Figure 1.

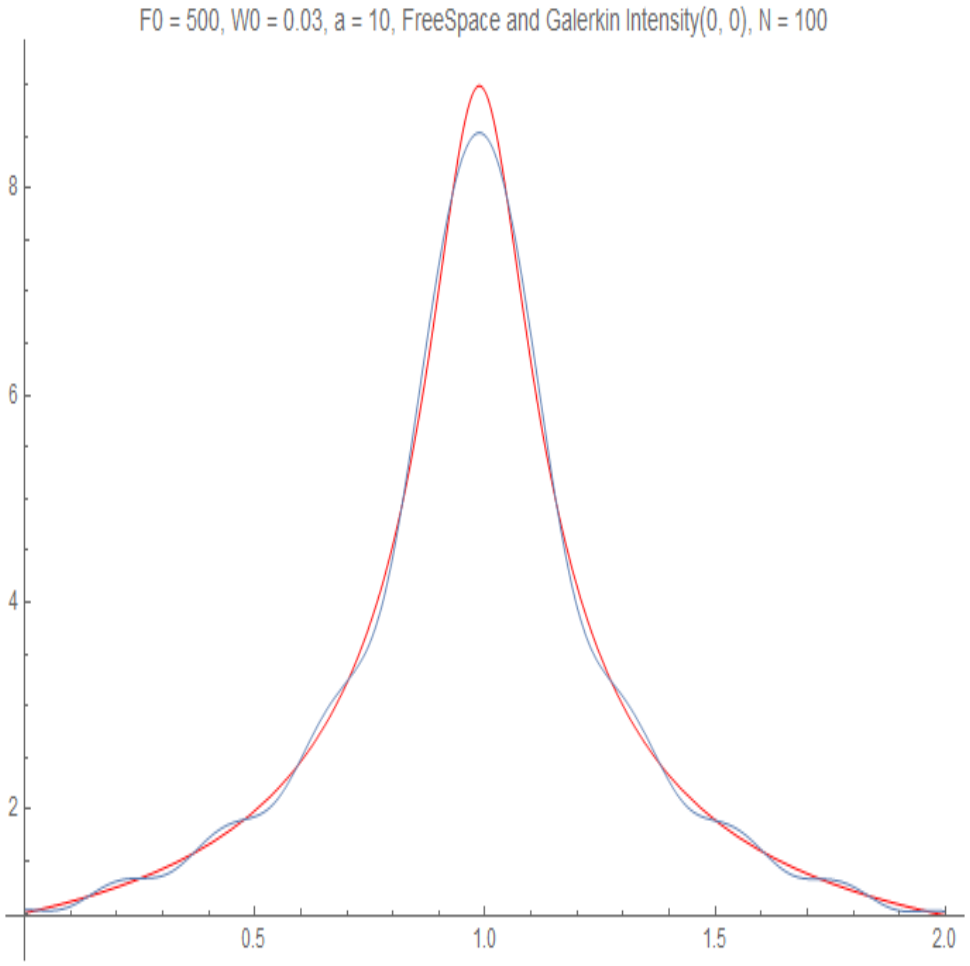

Figure 3: Similar to Figure 2, the two graphs in this figure are the graphs of the intensity, $|U|$.

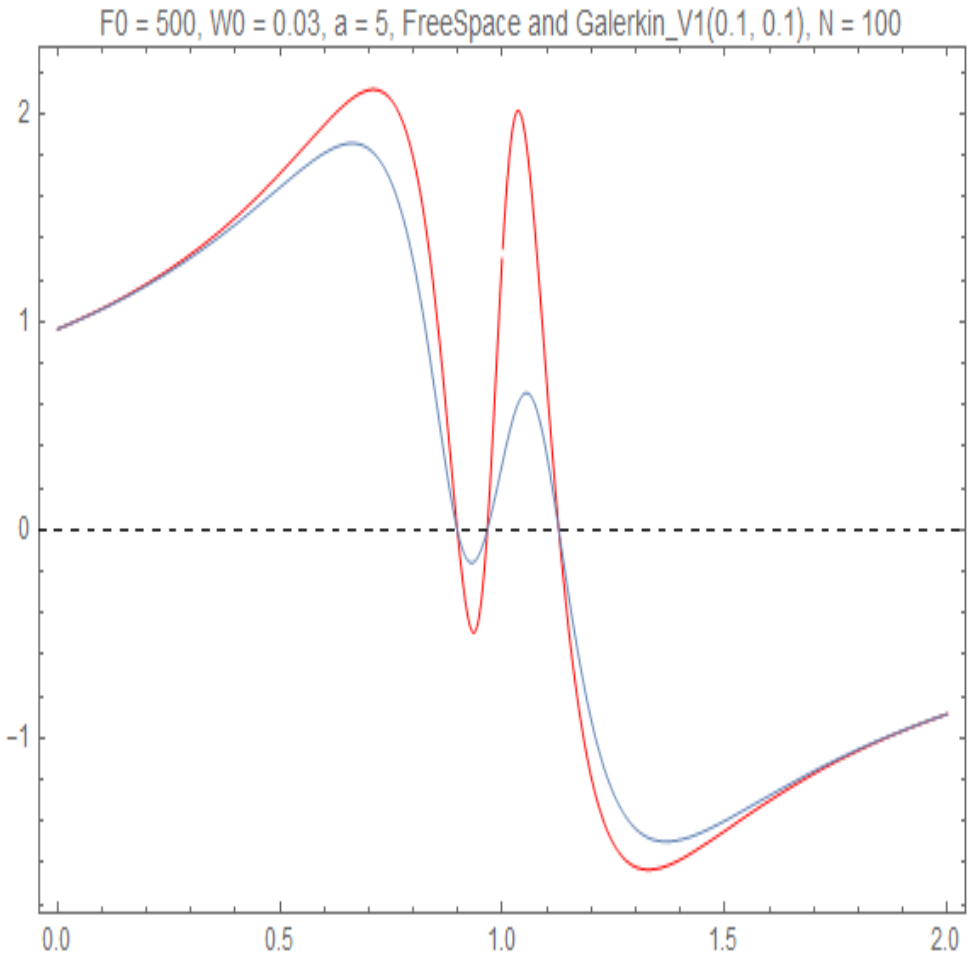

Figure 4: The Galerkin and free space solutions of V_1 at $(x, y) = (0.1, 0.1)$.

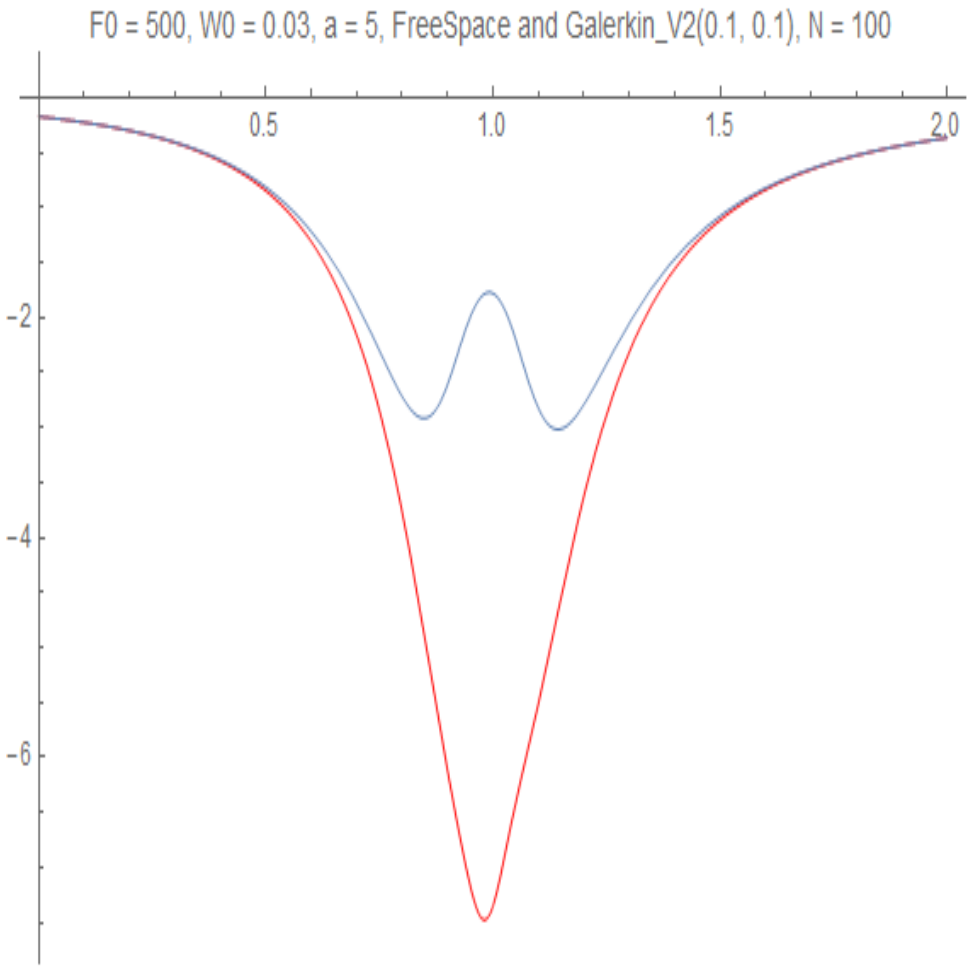

Figure 5: The Galerkin and free space solutions of V_2 at $(x, y) = (0.1, 0.1)$.

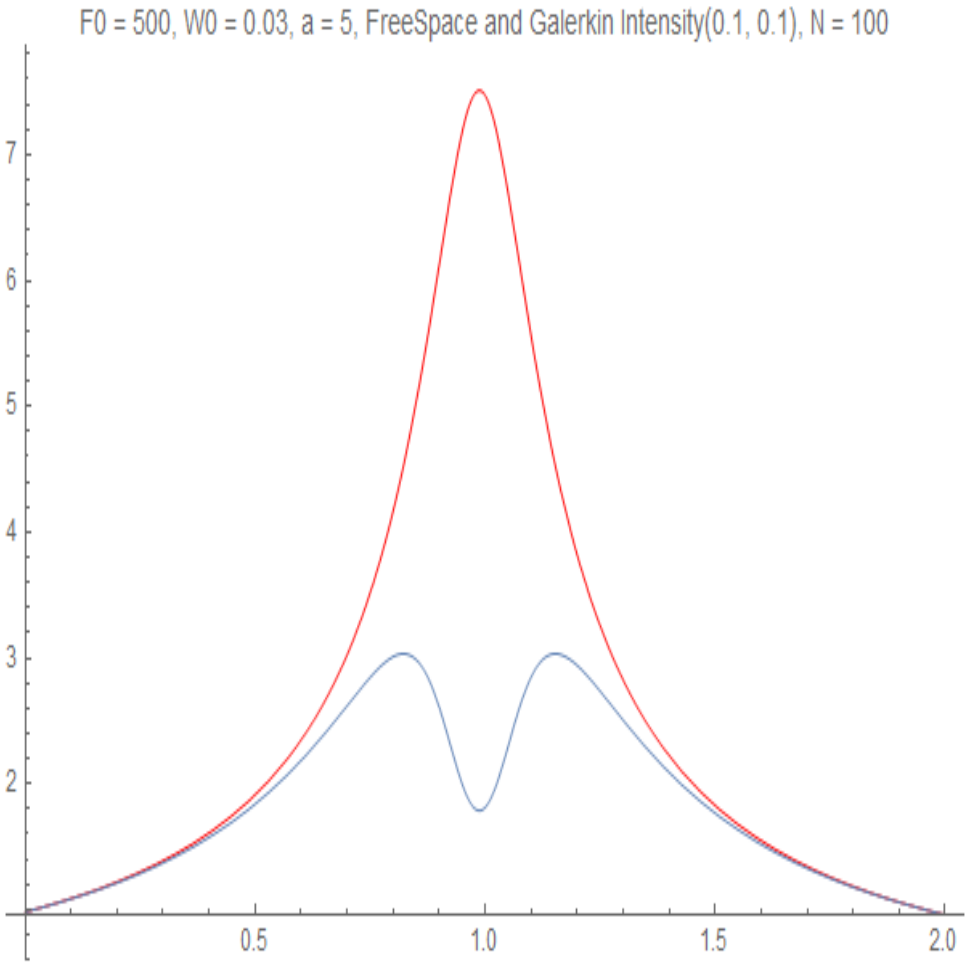

Figure 6: The Galerkin and free space solutions of the intensity $|U|$ at $(x, y) = (0.1, 0.1)$.

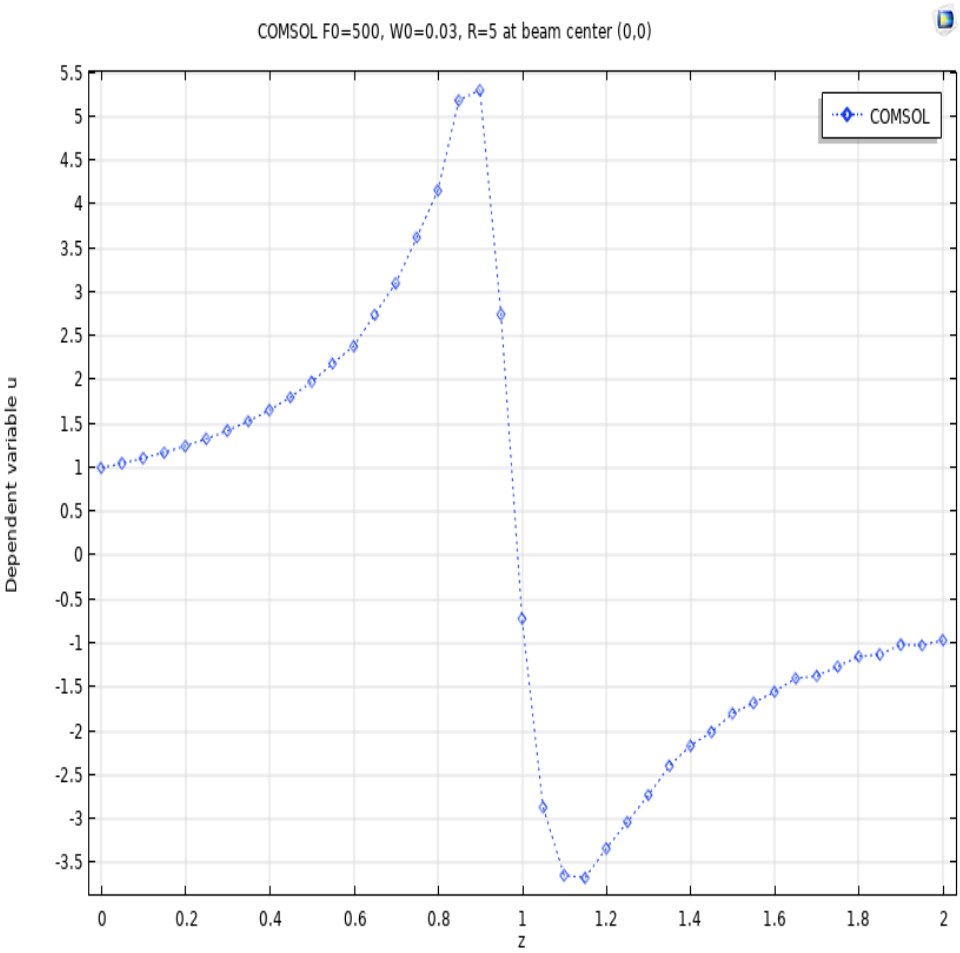

Figure 7: COMSOL result for V_1, corresponding to Figure 1.

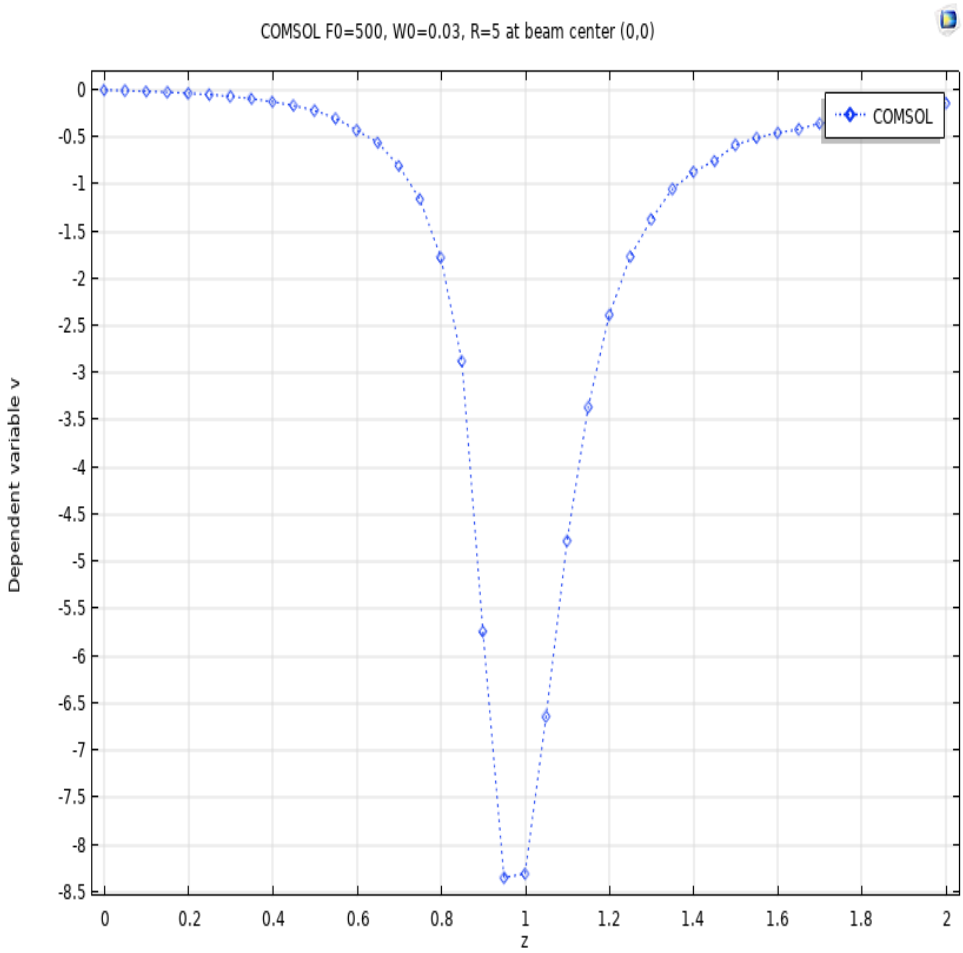

Figure 8: COMSOL result for V_2 corresponding to Figure 2.

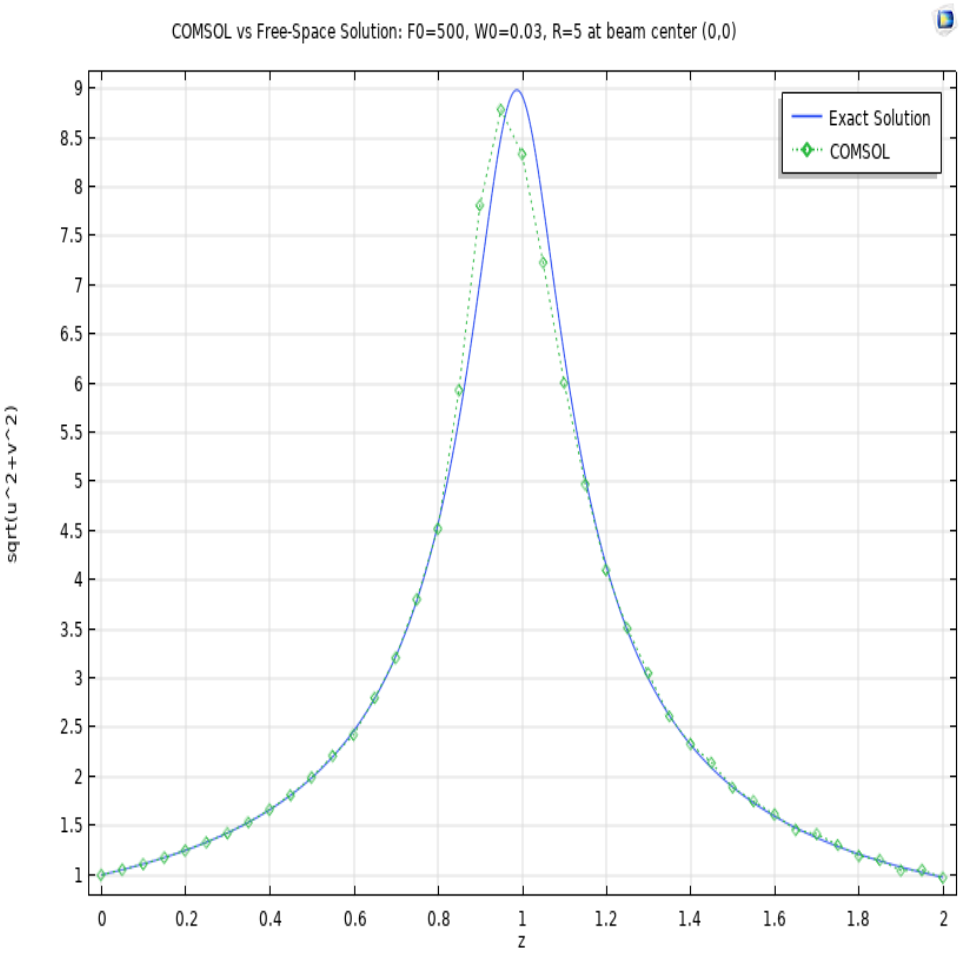

Figure 9: COMSOL result for $|U|$, corresponding to Figure 3

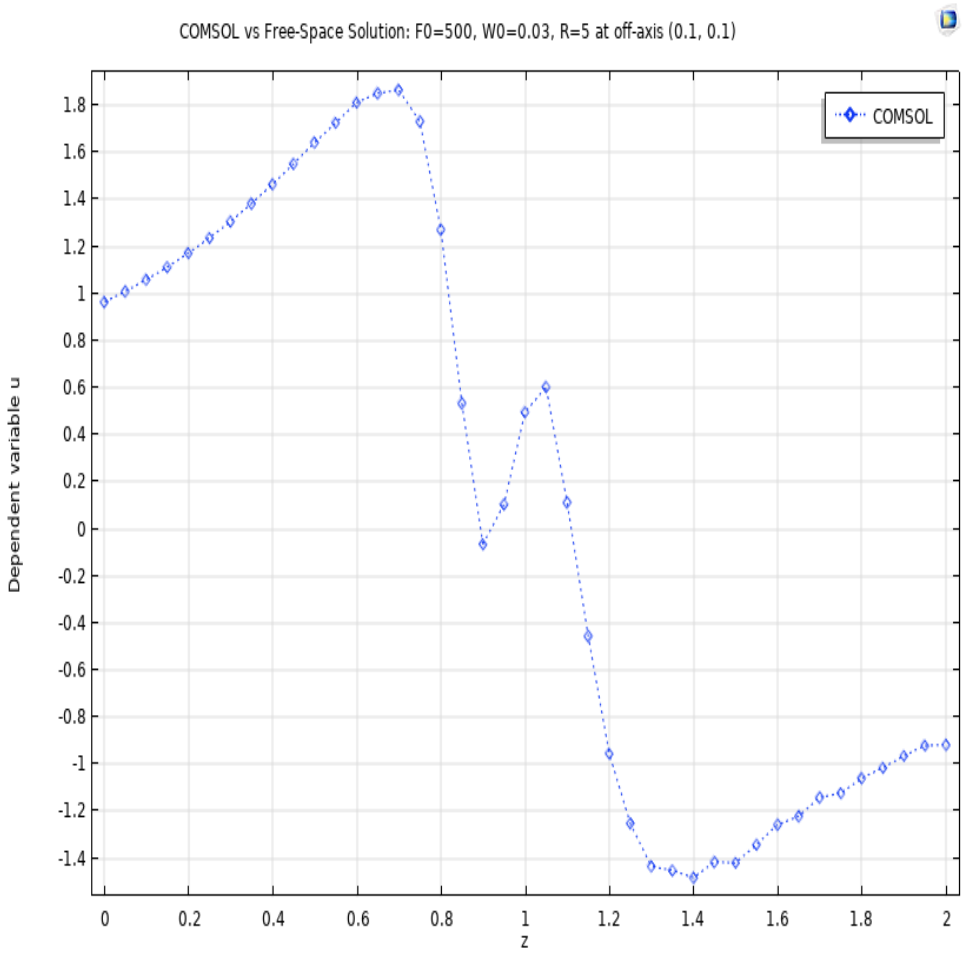

Figure 10: COMSOL result for V_1 at $(x, y) = (0.1, 0.1)$, corresponding to Figure 4..

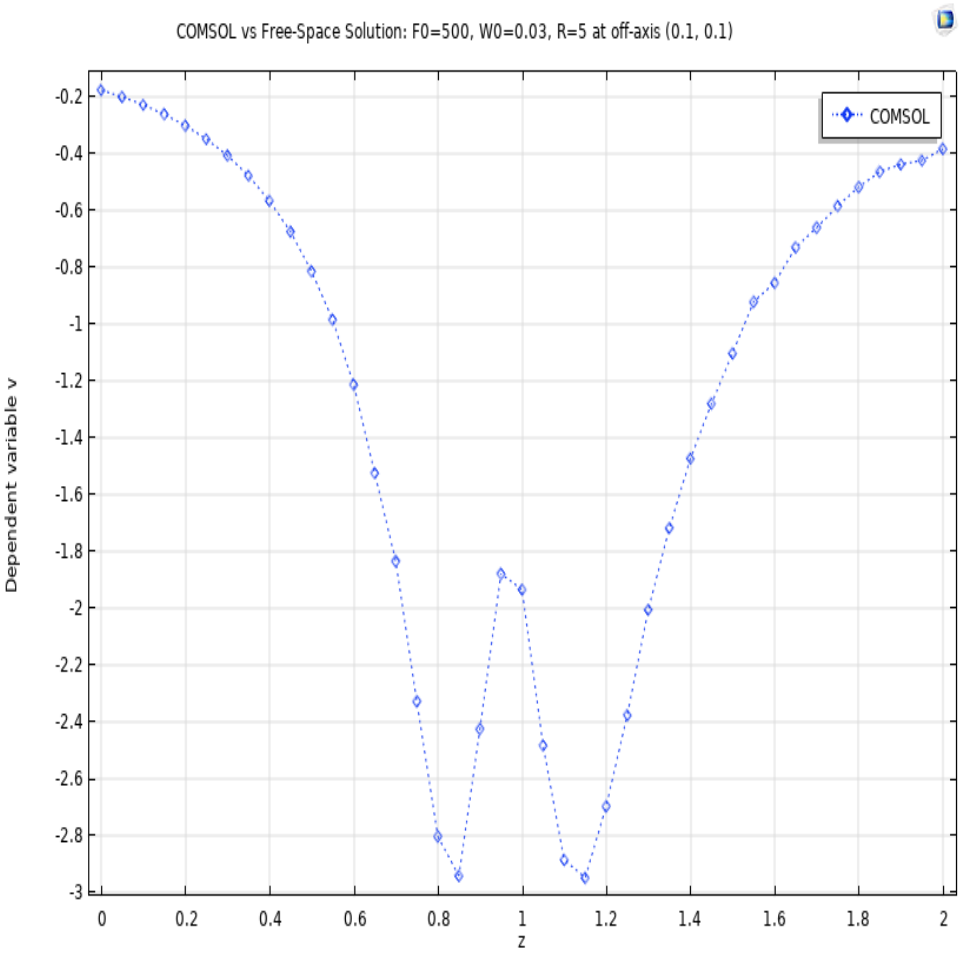

Figure 11: COMSOL result for V_2 at $(x, y) = (0.1, 0.1)$ corresponding to Figure 5.

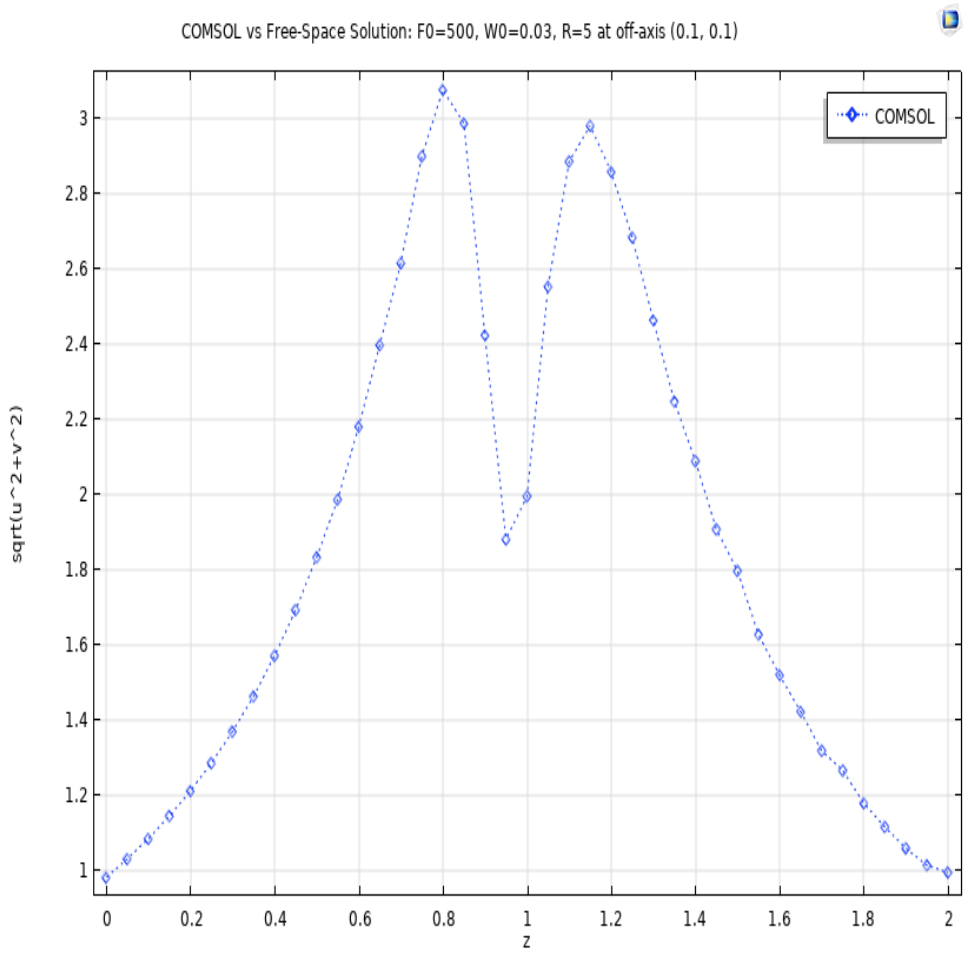

Figure 12: COMSOL result for $|U|$ at $(x, y) = (0.1, 0.1)$, corresponding to Figure 6.

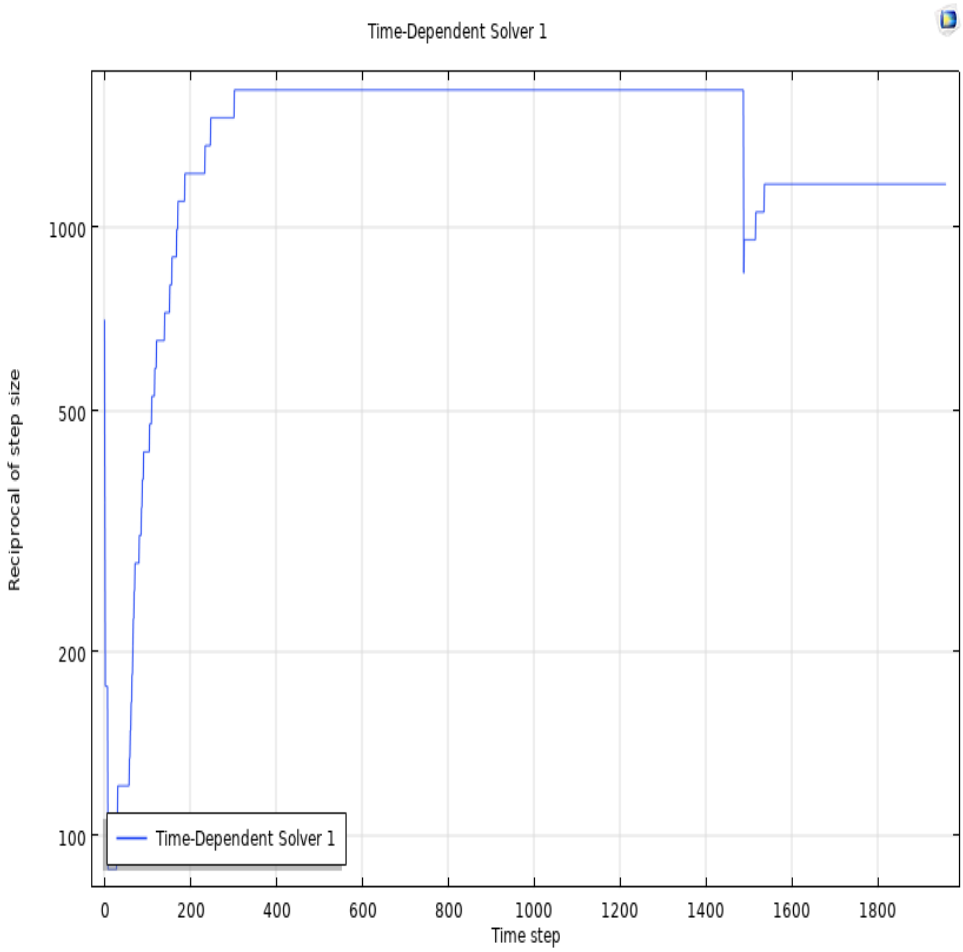

Figure 13: Convergence plot of COMSOL's Time-Dependent Solver.

References

[1] Larry C. Andrews, Ronald L. Phillips, Laser Beam Propagation through Random Media, SPIE, San Francisco, 2005.

[2] Svetlana Avramov-Zamurovic, Charles Nelson, Joel M. Esposito. Classification of beams carrying orbital angular momentum propagating through underwater turbulence, *Proc. SPIE 11532, Environmental Effects on Light Propagation and Adaptive Systems III, 115320D* (20 September 2020); doi: 10.1117/12.2572818